ELSEVIER

Comput. Methods Appl. Mech. Engrg. 126 (1995) 251–265

Computer methods in applied mechanics and engineering

Iterative method for the shape of static drops

Stanimir D. Iliev

Institute of Mechanics, Bulgarian Academy of Sciences, Akad. G. Bonchev Str. Bl. 4, 1113 Sofia, Bulgaria

Received 6 August 1993; revised 19 December 1994

Abstract

A numerical method for the computation of equilibrium shapes of liquid drops is presented. The latter are with fixed volume and undergo surface tension and gravity. An iterative procedure to minimize the energy of the system is used. A new scheme, which directly simulates virtual displacements of the considered system is described. The method is tested by studying a sessile drop and is used to analyze the equilibrium of a drop on an inclined plane handing from a square.

1. Introduction

The problems, involving the shape of static drops, occur in many scientific and technological areas. The configuration of free liquid surfaces in equilibrium under surface tension and gravity, is a solution of the generalized Plato problem and is of mathematical interest due to its non-linearity. The problem can be reduced to an ordinary differential equation only in the axisymmetric case. For this case the numerical approach (see [1, 2] and the references therein), an asymptotic approach [3] and the FEM approach to the Navier–Stokes equation with free surface [4] give good results. In a 3-D case the use of the asymptotical approach [5] is restricted to few special forms of the configuration. In [6], FEM is used to obtain the equilibrium shape of a drop contacting with an inclined plane over a circular wetted area. In the general case the use of FEM in 3-D is difficult since the structure of the drop shape and the boundary conditions can vary. Moreover, to fix the drop volume is one more problem.

In this paper we propose a numerical method in the 3-D space to obtain equilibrium shapes of liquid drop in a fluid. The drop has a fixed volume and is in contact with a set of rigid bodies. The numerical method is based on an iterative algorithm and variation formulation of the problem, and on the method [7] of generating a set of deformations of a drop with an arbitrary shape, consider volume and boundary conditions.

The general problem is formulated in Section 2. The numerical method of the general case is described in Section 3 and is tested in Section 4 for an equilibrium shape of a drop on a flat horizontal plane. Finally, in Section 5 the method is applied to calculate non-symmetrical equilibrium shapes of 'sessile-pendant' drops, i.e. liquid drop on the inclined plane, hanging from a square.

2. Formulation of the problem

The variation formulation of a drop equilibrium shape is a problem of how to find a configuration of a system which minimizes the system potential energy, considering given boundary and volume conditions.

We consider a material system, consisting of a simply connected incompressible liquid drop which occupies the domain Ω with volume V_0 in the fluid medium Ω_f. The drop is in contact with m ideal rigid

SSDI 0045-7825(95)00831-4

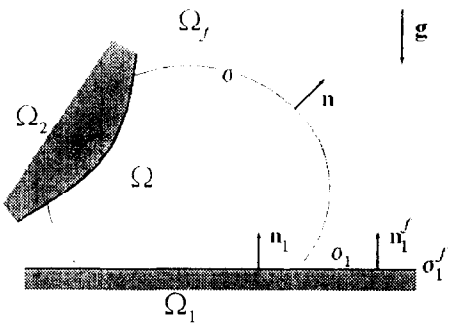

Fig. 1. Schematic drawing of the drop occupying domain Ω in the fluid medium Ω_f, contacted with ideal rigid bodies Ω_1, Ω_2, under the action of the gravity $\boldsymbol{g}$.

bodies $\Omega_1, \Omega_2, \ldots, \Omega_m$, and the surface tensions and gravity $\boldsymbol{g}$ act on the system—Fig. 1. Total potential energy Π of the system may be expressed by the following equation [8, 9]

$$\Pi = \int_{\Omega} \rho U \, \mathrm{d}\Omega + \int_{\Omega_f} \rho_f U \, \mathrm{d}\Omega_f + \int_{\Gamma} \sigma \, \mathrm{d}\Gamma + \sum_{i=1}^{m} \int_{\Gamma_i} \sigma_i \, \mathrm{d}\Gamma_i + \sum_{i=1}^{m} \int_{\Gamma_i^f} \sigma_i^f \, \mathrm{d}\Gamma_i^f . \tag{1}$$

Here, $\Gamma = \partial\Omega \cap \partial\Omega_f$, $\Gamma_i = \partial\Omega \cap \partial\Omega_i$, $\Gamma_i^f = \partial\Omega_f \cap \partial\Omega_i$, $\partial\Omega$, $\partial\Omega_f$, $\partial\Omega_1, \ldots, \partial\Omega_m$ are boundaries of the drop, fluid medium and rigid bodies; $\sigma, \sigma_1, \ldots, \sigma_m$, $\sigma_1^f, \ldots, \sigma_m^f$ are the surface tension coefficients at the interfaces $\Gamma, \Gamma_1, \ldots, \Gamma_m$, $\Gamma_1^f, \ldots, \Gamma_m^f$; ρ and ρ_f are local density of the liquid drop and fluid medium, correspondingly; U is the potential of the gravity force. In the present work we consider homogeneous and immiscible material, and domains $\Omega_1, \ldots, \Omega_m$ that are motionless.

In Eq. (1) it is seen that energy Π can be considered as a functional of drop and fluid medium domains Ω, Ω_f and of interfaces $\Gamma, \Gamma_1, \ldots, \Gamma_m$, $\Gamma_1^f, \ldots, \Gamma_m^f \ldots$, respectively. Therefore

$$\Pi = \Pi(\Omega, \Omega_f, \Gamma, \Gamma_1, \ldots, \Gamma_m, \Gamma_1^f, \ldots, \Gamma_m^f) \tag{2}$$

and the problem of obtaining an equilibrium shape is now reduced to the problem of minimizing the functional (2)

$$\Pi(\Omega, \Omega_f, \Gamma, \Gamma_1, \ldots, \Gamma_m, \Gamma_1^f, \ldots, \Gamma_m^f) \rightarrow \min , \tag{3}$$

subject to given volume and boundary conditions. The standard conditions are:

—*Volume conditions:* As a result of immiscibility we have

$$\delta \int_{\Omega} \mathrm{d}\Omega = -\delta \int_{\Omega_f} \mathrm{d}\Omega_f . \tag{4}$$

As a result of fluid drop incompressibility, the virtual displacements of the system must conserve the drop volume

$$V(\Omega) = \int_{\Omega} \mathrm{d}\Omega = V_0 = \text{const} . \tag{5}$$

Therefore, virtual displacements must satisfy the condition

$$\delta \int_{\Omega} \mathrm{d}\Omega = 0 . \tag{6}$$

—*Boundary conditions:* As a result of immiscibility, the virtual displacements $\delta \boldsymbol{r}_i$ and $\delta \boldsymbol{r}_i^f$ of the boundary fluid elements $\boldsymbol{r}_i \in \Gamma_i$, $i = 1, \ldots, m$ and $\delta \boldsymbol{r}_i^f$, $\boldsymbol{r}_i^f \in \Gamma_i^f$, $i = 1, \ldots, m$ must satisfy conditions

$$(\delta \boldsymbol{r}_i \cdot \boldsymbol{n}_i) \geq 0 , \quad \boldsymbol{r}_i \in \Gamma_i , \quad i = 1, \ldots, m . \tag{7.1}$$

$$(\delta \boldsymbol{r}_i^f \cdot \boldsymbol{n}_i) \geqslant 0\,, \quad \boldsymbol{r}_i^f \in \Gamma_i^f\,, \quad i = 1, \ldots, m\,. \tag{7.2}$$

Here, $\boldsymbol{n}_i$ is the unit outward normal to Ω_i at $\boldsymbol{r}_i$ or $\boldsymbol{r}_i^f$, correspondingly. To conserve the areas of rigid body surfaces, virtual displacements must satisfy conditions

$$\delta \int_{\Gamma_i} \mathrm{d}\Gamma_i = -\delta \int_{\Gamma_i^f} \mathrm{d}\Gamma_i^f\,, \quad i = 1, \ldots, m\,. \tag{8}$$

The problem is now to minimize the functional (2), subject to conditions (4)–(8). In the special cases, additional conditions for the solid boundaries can be defined. For example, the contact surface between the drop and some rigid bodies is fixed or can be localized in a definite region.

As a result of (4) and (8), the configuration of the system which minimizes the functional (2) with conditions (4)–(8) also minimizes the functional

$$\bar{\Pi} = \bar{\Pi}(\Omega, \Gamma, \Gamma_1, \ldots, \Gamma_m) = \int_\Omega \frac{(\rho - \rho_f)}{\sigma} U \,\mathrm{d}\Omega + \int_\Gamma \mathrm{d}\Gamma + \sum_{i=1}^{m} \int_{\Gamma_i} \frac{(\sigma_i - \sigma_i^f)}{\sigma} \mathrm{d}\Gamma_i \tag{9}$$

with conditions (5), (6) and (7.1). Therefore, to obtain the equilibrium shape we can use the functional (9). It is clear that interfaces $\Gamma_i, i = 1, \ldots, m$ are determined by Γ and $\partial\Omega_i, i = 1, \ldots, m$. The liquid drop domain Ω is uniquely determined by frontiers $\Gamma, \partial\Omega_1, \ldots, \partial\Omega_m$. Since rigid bodies are motionless, surfaces $\partial\Omega_i, i = 1, \ldots, m$ in the functional (9) are fixed and not variables. Therefore, we have that there is only one independent variable in the functional (9), and it is Γ

$$\bar{\Pi} = F(\Omega(\Gamma \| \partial\Omega_1, \ldots, \partial\Omega_m), \Gamma \| \partial\Omega_1, \ldots, \partial\Omega_m)\,,$$

However, other terms may be uniquely reconstructed, but this does not mean that functional may be reduced to the boundary problem.

Introduce Cartesian coordinate system (x, y, z), where

$$z = -\boldsymbol{g}/\|\boldsymbol{g}\|\,.$$

and assume that gravity potential is given as $U = gz$, where g is gravity acceleration. Setting

$$b = \frac{(\rho - \rho_f)g}{\sigma}\,, \qquad \chi_i = \frac{(\sigma_i - \sigma_i^f)}{\sigma}\,, \quad i = 1, \ldots, m\,. \tag{10}$$

The functional (9) is reduced to:

$$\bar{\Pi} = F(\Omega(\Gamma \| \partial\Omega_1, \ldots, \partial\Omega_m), \Gamma \| \partial\Omega_1, \ldots, \partial\Omega_m) = \int_\Omega bz \,\mathrm{d}\Omega(\Gamma \| \partial\Omega_1, \ldots, \partial\Omega_m)$$
$$+ \int_\Gamma \mathrm{d}\Gamma + \sum_{i=1}^{m} \int_{\Gamma_i} \chi_i \,\mathrm{d}\Gamma_i(\Gamma \| \partial\Omega_1, \ldots, \partial\Omega_m) \tag{11}$$

Then finally, the problem to obtain equilibrium shape is finally reduced to:

PROBLEM $\mathcal{T}$. For the set of the fixed solid surfaces $\partial\Omega_i, i = 1, \ldots, m$ find a surface in 3-D contacting with surfaces $\partial\Omega_i, i = 1, \ldots, m$, so that the latter bound a domain Ω with volume V_0 and minimize the functional (11), subject to given conditions (6) and (7.1).

For the set of fixed solid surfaces $\partial\Omega_i, i = 1, \ldots, m$, the problem parameters are

$$V_0, b, \chi_1, \ldots, \chi_m\,. \tag{12}$$

In some cases a reference length L can exist. The natural length scale of our problem is the capillary length given by $a = 1/\sqrt{b}, m^{-1}$. We make (11) dimensionless as follows

$$X = \frac{x}{aL}\,, \qquad Y = \frac{y}{aL}\,, \qquad Z = \frac{z}{aL}$$

REMARK 1. Equilibrium shapes can be obtained as a solution of the equations

$$\delta F = 0\,, \tag{13}$$

(5), (6) and (7.1), yielding the well-known Laplace capillary equation

$$(1/R_1(\boldsymbol{r}) + 1/R_2(\boldsymbol{r})) = bz + C\,, \qquad C = \text{const}\,, \quad \text{for } \boldsymbol{r} \in \Gamma\,, \tag{14}$$

and equations

$$\boldsymbol{n}(\boldsymbol{r}_i) \cdot \boldsymbol{n}_i(\boldsymbol{r}_i) = \chi_i \quad \text{for } \boldsymbol{r}_i \in \partial\Gamma \cap \partial\Omega_i \quad i = 1, \ldots, m\,. \tag{15}$$

3. Numerical method

The numerical method of solving the variation Problem $\mathcal{T}$ is successively given by the following algorithm. The algorithm starts with an approximation of an arbitrary possible configuration $(\{\Omega^0, \Gamma^0, \partial\Omega_i, i = 1, \ldots, m\}$, which gives volume and boundary conditions and iteratively generates the sequence of finite deformations $\Omega^i, \Gamma^i, i = 1, 2, 3, \ldots$ and the configuration gives conditions (6), (7.1), satisfying $F(\Omega^{i-1}, \Gamma^{i-1}) > F(\Omega^i, \Gamma^i)$. Before describing the algorithm in detail, let us describe the numerical realization of each of its components.

3.1. Approximation of Γ and Ω

An arbitrary surface Γ in 3-D space in the presented method is discretized by a set of triangles. Denote the obtained triangulation of Γ by $\bar{\Gamma}$

$$\bar{\Gamma} = \bigcup_{j=1}^{M} e^j = e^1(\boldsymbol{p}^{j_1}, \boldsymbol{p}^{j_2}, \boldsymbol{p}^{j_3}) \cup e^2(\boldsymbol{p}^{2_1}, \boldsymbol{p}^{2_2}, \boldsymbol{p}^{2_3}) \cup \cdots \cup e^M(\boldsymbol{p}^{M_1}, \boldsymbol{p}^{M_2}, \boldsymbol{p}^{M_3})\,. \tag{16}$$

Here, e^j is the triangle with nodes $\boldsymbol{p}^{j_1}, \boldsymbol{p}^{j_2}, \boldsymbol{p}^{j_3}$. Assume that there are N nodes $\boldsymbol{p}^1, \boldsymbol{p}^2, \ldots, \boldsymbol{p}^N$ on $\bar{\Gamma}$, where N_1 nodes are interal with respect to the domain $\bar{\Gamma}$. Let they be nodes $\boldsymbol{p}^1, \boldsymbol{p}^2, \ldots, \boldsymbol{p}^{N_1}$

$$\boldsymbol{p}^i \in \partial\bar{\Gamma}\,, \quad i = 1, \ldots, N_1\,, \tag{17.1}$$

while the other nodes $\boldsymbol{p}^{N_1+1}, \boldsymbol{p}^{N_1+2}, \ldots, \boldsymbol{p}^N$ be boundaries

$$\boldsymbol{p}^{N_1+1}, \ldots, \boldsymbol{p}^{N_2} \in \partial\bar{\Gamma} \cap \partial\Omega_1, \ldots, \boldsymbol{p}^{N_m+1}, \ldots, \boldsymbol{p}^N \in \partial\bar{\Gamma} \cap \partial\Omega_m\,. \tag{17.2}$$

We have that

$$\bar{\Gamma} = \bar{\Gamma}(e^1, \ldots, e^M) = \bar{\Gamma}(\boldsymbol{p}^1, \ldots, \boldsymbol{p}^N)\,. \tag{18}$$

$\bar{\Gamma}$ and the set $\partial\Omega_i, i = 1, \ldots, m$ determines the approximation $\bar{\Omega}(\bar{\Gamma} \| \partial\Omega_1, \ldots, \partial\Omega_m)$ of the drop domain Ω.

3.2. Approximation of the virtual displacements

The virtual displacements of an arbitrary configuration

$$\{\bar{\Gamma}, \partial\Omega_i, i = 1, \ldots, m, \bar{\Omega}(\bar{\Gamma} \| \partial\Omega_1, \ldots, \partial\Omega_m)\}$$

are determined by the finite displacements of the surface $\bar{\Gamma}$, as a result of which surface $\bar{\Gamma}$ passes into $\bar{\Gamma}_\Delta$ and domain $\bar{\Omega}(\bar{\Gamma} \| \partial\Omega_1, \ldots, \partial\Omega_m)$ passes into $\bar{\Omega}_\Delta(\bar{\Gamma}_\Delta \| \partial\Omega_1, \ldots, \partial\Omega_m)$. And now for the virtual displacements $\bar{\Gamma}_\Delta$, of $\bar{\Gamma}$ we can write

$$\begin{aligned}\bar{\Gamma}_\Delta = \bigcup_{j=1}^{M} e^j_\Delta = {} & e^1(\boldsymbol{p}^{1_1} + \Delta\boldsymbol{p}^{1_1}, \boldsymbol{p}^{1_2} + \Delta\boldsymbol{p}^{1_2}, \boldsymbol{p}^{1_3} + \Delta\boldsymbol{p}^{1_3}) \\ & \cup e^2(\boldsymbol{p}^{2_1} + \Delta\boldsymbol{p}^{2_1}, \boldsymbol{p}^{2_2} + \Delta\boldsymbol{p}^{2_2}, \boldsymbol{p}^{2_3} + \Delta\boldsymbol{p}^{2_3}) \cup \cdots \cup \\ & \cup e^M(\boldsymbol{p}^{M_1} + \Delta\boldsymbol{p}^{M_1}, \boldsymbol{p}^{M_2} + \Delta\boldsymbol{p}^{M_2}, \boldsymbol{p}^{M_3} + \Delta\boldsymbol{p}^{M_3})\end{aligned} \tag{19}$$

Here, displacements $\Delta\boldsymbol{p}^i, i = 1, \ldots, N$ of nodes $\boldsymbol{p}^i, \boldsymbol{p}^i \in \bar{\Gamma}, i = 1, \ldots, N$ are determined as

$$\Delta \boldsymbol{p}^i = \varepsilon_i \boldsymbol{N}_i\,, \qquad \|\boldsymbol{N}_i\| = 1\,, \quad i = 1, \ldots, N\,. \tag{20}$$

As a result of displacements (20) nodes $\boldsymbol{p}^i$ pass into $\boldsymbol{p}^i_\Delta$

$$\boldsymbol{p}^i_\Delta = \boldsymbol{p}^i + \Delta \boldsymbol{p}^i\,, \quad i = 1, \ldots, N\,, \tag{21}$$

triangles $e^i(\boldsymbol{p}^{i_1}, \boldsymbol{p}^{i_2}, \boldsymbol{p}^{i_3}), i = 1, \ldots, M$ pass into triangles $e^i_\Delta = e^i(\boldsymbol{p}^{i_1}_\Delta, \boldsymbol{p}^{i_2}_\Delta, \boldsymbol{p}^{i_3}_\Delta)$. We have that

$$\begin{aligned}\bar{\Gamma}_\Delta &= \bar{\Gamma}_\Delta(\bar{\Gamma}, \boldsymbol{p}^1_\Delta, \boldsymbol{p}^2_\Delta, \ldots, \boldsymbol{p}^N_\Delta) = \bar{\Gamma}_\Delta(\bar{\Gamma}, \varepsilon_1, \ldots, \varepsilon_N, \boldsymbol{N}_1, \ldots, \boldsymbol{N}_N) \\ &= \bar{\Gamma}_\Delta(\boldsymbol{p}^1, \boldsymbol{p}^2, \ldots, \boldsymbol{p}^N, \varepsilon_1, \ldots, \varepsilon_N, \boldsymbol{N}_1, \ldots, \boldsymbol{N}_N)\,.\end{aligned} \tag{22}$$

3.3. Approximation of the boundary and volume conditions by the configuration $\{\bar{\Gamma}, \partial\Omega_i, i = 1, \ldots, m, \bar{\Omega}(\bar{\Gamma}\|\partial\Omega_1, \ldots, \partial\Omega_m)\}$

To approximate the boundary conditions (7.1), displacements (20) must satisfy equations

$$[\boldsymbol{p}^i, \boldsymbol{p}^i_\Delta] \cap \partial\Omega_j = \emptyset\,, \quad i = 1, \ldots, N_1\,, \quad j = 1, \ldots, m\,, \tag{23.1}$$

$$p^i_\Delta \in \bigcup_{j=1}^{m} \partial\Omega_j\,, \quad i = N_1 + 1, \ldots, N\,. \tag{23.2}$$

Condition

$$\Delta V = V(\bar{\Gamma}_\Delta) - V(\bar{\Gamma}) = 0 \tag{24}$$

approximates the volume condition (6).

3.4. Calculation of ΔF *and* ΔV

By determining in this way $\bar{\Gamma}, \bar{\Omega}(\bar{\Gamma}\|\partial\Omega_1, \ldots, \partial\Omega_m), \partial\Omega_i, i = 1, \ldots, m, \bar{\Gamma}_\Delta, \bar{\Omega}_\Delta(\bar{\Gamma}_\Delta\|\partial\Omega_1, \ldots, \partial\Omega_m), \Delta F$ is determined as

$$\Delta F = F(\bar{\Gamma}_\Delta) - F(\bar{\Gamma})\,.$$

The so-determined ΔF and ΔV depend on $\boldsymbol{p}^1, \boldsymbol{p}^2, \ldots, \boldsymbol{p}^N, \varepsilon_1, \ldots, \varepsilon_N, \boldsymbol{N}_1, \ldots, \boldsymbol{N}_N$. We have

$$\begin{aligned}&\Delta F = \Delta F(\boldsymbol{p}^1, \boldsymbol{p}^2, \ldots, \boldsymbol{p}^N, \varepsilon_1, \ldots, \varepsilon_N, \boldsymbol{N}_1, \ldots, \boldsymbol{N}_N)\,, \\ &\Delta V = V(\bar{\Gamma}_\Delta) - V(\bar{\Gamma}) = \Delta V(\boldsymbol{p}^1, \boldsymbol{p}^2, \ldots, \boldsymbol{p}^N, \varepsilon_1, \ldots, \varepsilon_N, \boldsymbol{N}_1, \ldots, \boldsymbol{N}_N) = 0\,.\end{aligned}$$

In our numerical method we calculate ΔF and ΔV, using formulas from analytical geometry for the area, volume and mass center.

We shall consider at first, finite deformation of the surface $\bar{\Gamma}$ in which only one

$$\varepsilon_q \neq 0\,, \quad 0 \leq q \leq N\,, \quad \varepsilon_i = 0\,, \quad i = 1, \ldots, q-1\,, \quad q+1, \ldots, N\,.$$

We have that $\bar{\Gamma}_\Delta = \bar{\Gamma}_\Delta(\bar{\Gamma}, \varepsilon_q, \boldsymbol{N}_q)$. Let $\boldsymbol{p}^q$ be a node of triangles

$$e^{q_1} \in \bar{\Gamma}, \ldots, e^{q_l} \in \bar{\Gamma} \tag{25}$$

with nodes

$$\boldsymbol{p}^q, \boldsymbol{p}^{q_1}, \boldsymbol{p}^{q_2}, \ldots, \boldsymbol{p}^{q_l}\,. \tag{26}$$

Renumber the nodal points (26) into

$$\boldsymbol{p}, \boldsymbol{p}^1, \boldsymbol{p}^2, \ldots, \boldsymbol{p}^l \tag{27}$$

such, that conditions

(1) $[\boldsymbol{p}^l, \boldsymbol{p}^1] \subset \bar{\Gamma}, [\boldsymbol{p}^1, \boldsymbol{p}^2] \subset \bar{\Gamma}, \ldots, [\boldsymbol{p}^{l-w-1}, \boldsymbol{p}^{l-w}] \subset \bar{\Gamma}\,,$
$[\boldsymbol{p}^{l-w}, \boldsymbol{p}^{l-w+1}] \subset \partial\bar{\Gamma}, \ldots, [\boldsymbol{p}^{l-1}, \boldsymbol{p}^l] \subset \partial\bar{\Gamma}\,, \quad 0 \leq w < l$

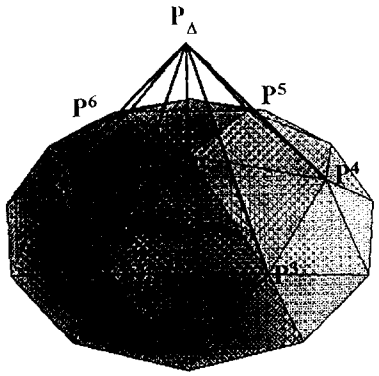

Fig. 2. Deformation of the surface as the result of the displacement of one node. Here, $p_\Delta = p + 0.2n^q$.

be satisfied.

(2) vectors $b^1, \ldots, b^{l-1}, b^l$ must be directed into $\Omega(\bar{\Gamma} \| \partial\Omega_1, \ldots, \partial\Omega_m)$ (see Fig. 2). Here

$$b^1 = a^1 \times a^2, \ldots, b^{l-1} = a^{l-1} \times a^l, \qquad b^l = a^l \times a^1, \tag{28.1}$$

$$a^i = p - p^i, \quad i = 1, \ldots, l. \tag{28.2}$$

Let nodes $p^1, p^2, \ldots, p^w$ be interior for domain $\bar{\Gamma}$, and other nodes $p^{w+1}, p^{w+2}, \ldots, p^l$ be boundaries

$$p^i \in \partial\bar{\Gamma} \cap \partial\Omega_j, \quad i = w+1, \ldots, l, \quad 0 \leq w < l, \quad 1 \leq j \leq m.$$

We have that

$$\Delta F(\bar{\Gamma}, \varepsilon_q, N_q) = z_{\text{mass}}\, \Delta V(\bar{\Gamma}, \varepsilon_q, N_q) + \Delta(\bar{\Gamma}, \varepsilon_q, N_q) + \chi_j\, \Delta_j(\bar{\Gamma}, \varepsilon_q, N_q). \tag{29}$$

Here

$$\Delta V = \varepsilon_q \frac{1}{6}((b^1_\Delta + \cdots + b^{l-1}_\Delta + b^l_\Delta) \cdot N_q), \tag{30.1}$$

$$\Delta = \begin{cases} \frac{1}{2}((\|b^l_\Delta\| - \|b^l\|) + (\|b^1_\Delta\| - \|b^1\|) + \cdots + (\|b^w_\Delta\| - \|b^w\|)), & \text{if } w < l, \\ \frac{1}{2}((\|b^1_\Delta\| - \|b^1\|) + \cdots + (\|b^l_\Delta\| - \|b^l\|)), & \text{if } w = l, \end{cases} \tag{30.2}$$

$$\Delta_j = \begin{cases} \frac{1}{2}((\|b^{w+1}_\Delta\| - \|b^{w+1}\|) + \cdots + (\|b^{l-1}_\Delta\| - \|b^{l-1}\|)), & \text{if } w < l, \\ 0, & \text{if } w = l, \end{cases} \tag{30.3}$$

z_{mass} is z coordinate of the mass center of a polyhedron with nodes $p, p^1, \ldots, p^l, p^q_\Delta$,

$$b^1_\Delta = a^1_\Delta \times a^2_\Delta, \ldots, b^{l-1}_\Delta = a^{l-1}_\Delta \times a^l_\Delta, \qquad b^l_\Delta = a^l_\Delta \times a^1_\Delta, \tag{31.1}$$

$$a^i_\Delta = p^q_\Delta - p^i, \quad i = 1, \ldots, l. \tag{31.2}$$

In the general case (22) in which $\varepsilon_i \neq 0, i = 1, \ldots, N$ deformation

$$\bar{\Gamma}_\Delta = \bar{\Gamma}_\Delta(\bar{\Gamma}, \varepsilon_1, \ldots, \varepsilon_N, N_1, \ldots, N_N)$$

is equivalent to the sum of N one-node deformations. We have

$$\bar{\Gamma}_\Delta(\bar{\Gamma}, \varepsilon_1, \ldots, \varepsilon_N, N_1, \ldots, N_N) = \bar{\Gamma}_\Delta(\bar{\Gamma}_\Delta(\bar{\Gamma}, \varepsilon_q, N_q), \varepsilon_1, \ldots, \varepsilon_{q-1}, \varepsilon_{q+1}, \ldots, \varepsilon_N, N_1, \ldots, N_{q-1}, N_{q+1}, \ldots, N_N)$$

for an arbitrary $q \in \{1, \ldots, N\}$. Therefore

$$\Delta F(\boldsymbol{p}^1, \ldots, \boldsymbol{p}^N, \varepsilon_1 N_1, \ldots, \varepsilon_N N_N) = \Delta F(\boldsymbol{p}^1, \boldsymbol{p}^2_\Delta, \ldots, \boldsymbol{p}^N_\Delta, \varepsilon_1 N_1(\ldots(\boldsymbol{p}^1, \ldots, \boldsymbol{p}^N, \varepsilon_N N_N)))$$
$$= \Delta F(\boldsymbol{p}^1, \boldsymbol{p}^2_\Delta, \ldots, \boldsymbol{p}^N_\Delta, \varepsilon_1 N_1(\ldots \varepsilon_i N_i(\ldots \varepsilon_j N_j(\ldots(\boldsymbol{p}^1, \ldots, \boldsymbol{p}^N, \varepsilon_N N_N)))))$$
$$= \Delta F(\boldsymbol{p}^1, \boldsymbol{p}^2_\Delta, \ldots, \boldsymbol{p}^N_\Delta, \varepsilon_1 N_1(\ldots \varepsilon_j N_j(\ldots \varepsilon_i N_i(\ldots(\boldsymbol{p}^1, \ldots, \boldsymbol{p}^N, \varepsilon_N N_N))))) ,$$

$$\Delta V(\boldsymbol{p}^1, \ldots, \boldsymbol{p}^N, \varepsilon_1 N_1, \ldots, \varepsilon_N N_N) = \Delta V(\boldsymbol{p}^1, \boldsymbol{p}^2_\Delta, \ldots, \boldsymbol{p}^N_\Delta, \varepsilon_1 N_1(\ldots(\boldsymbol{p}^1, \ldots, \boldsymbol{p}^N, \varepsilon_N N_N)))$$
$$= \Delta V(\boldsymbol{p}^1, \boldsymbol{p}^2_\Delta, \ldots, \boldsymbol{p}^N_\Delta, \varepsilon_1 N_1(\ldots \varepsilon_i N_i(\ldots \varepsilon_j N_j(\ldots(\boldsymbol{p}^1, \ldots, \boldsymbol{p}^N, \varepsilon_N N_N)))))$$
$$= \Delta V(\boldsymbol{p}^1, \boldsymbol{p}^2_\Delta, \ldots, \boldsymbol{p}^N_\Delta, \varepsilon_1 N_1(\ldots \varepsilon_j N_j(\ldots \varepsilon_i N_i(\ldots(\boldsymbol{p}^1, \ldots, \boldsymbol{p}^N, \varepsilon_N N_N))))) ,$$

for arbitrary $i, j \in \{1, \ldots, N\}, i \neq j$. To calculate ΔF and ΔV we can use the results of the case of one-node deformation.

3.5. *Approximation of the set of ε possible deformations of $\bar{\Gamma}$*

Let $\bar{\Gamma}$ consist of a set of N triangles. For fixed $\varepsilon > 0$ we can define the set of ε possible deformations $\{\bar{\Gamma}_\Delta\}$ of $\bar{\Gamma}$ in different ways.

(1) A set of unit radius vectors

$$\left\{N(I, J) = \left(\sin\frac{I\pi}{K}\cos\frac{J2\pi}{K}, \sin\frac{I\pi}{K}\sin\frac{J2\pi}{K}, \cos\frac{I\pi}{K}\right): 0 \leq I, J \leq K\right\} \tag{32}$$

and set

$$\{(\varepsilon_1 = \pm\varepsilon, \ldots, \varepsilon_{q-1} = \pm\varepsilon, \varepsilon_q, \varepsilon_{q+1} = \pm\varepsilon, \ldots, \varepsilon_N = \pm\varepsilon), q = 1, \ldots, N\} , \tag{33}$$

where

$$\varepsilon_q = \frac{6(\Delta V(\bar{\Gamma}, \varepsilon_1, \ldots, \varepsilon_{q-1}, \varepsilon_{q+1}, \ldots, \varepsilon_N, N_1, \ldots, N_{q-1}, N_{q+1}, \ldots, N_N) - V_0)}{(\boldsymbol{b}^1_\Delta + \cdots + \boldsymbol{b}^{l-1}_\Delta + \boldsymbol{b}^l_\Delta)\cdot N_q} , \tag{34}$$

and $\boldsymbol{b}^1, \ldots, \boldsymbol{b}^l$ satisfy (26), (27), (31.1), determining the finite set of deformations

$$\{\Delta\boldsymbol{p}^i = \varepsilon_i N_i, \quad i = 1, \ldots, N\}$$

of the nodes and a set of deformations of the surface $\bar{\Gamma}$, conserving volume of the drop. K and ε are parameters of this set. The condition that these deformations be possible is that they satisfy conditions (23). Denote by $\Psi_1^{\varepsilon,K}(\bar{\Gamma})$ a set of possible deformations of $\bar{\Gamma}$ determined by the conditions (32)–(34), (23).

(2) Vector

$$\boldsymbol{n}^q = (\boldsymbol{b}^1 + \cdots + \boldsymbol{b}^l)/\|\boldsymbol{b}^1 + \cdots + \boldsymbol{b}^l\| , \tag{35}$$

where $\boldsymbol{b}^1, \ldots, \boldsymbol{b}^l$ satisfy (26)–(28), approximates the unit outnormal to the surface Γ in $\boldsymbol{p}^q$. We can use the set $\Psi_2^\varepsilon(\bar{\Gamma})$ of possible deformations determined by a set

$$\{\Delta\boldsymbol{p}^i = \varepsilon_i \boldsymbol{n}^i, \quad i = 1, \ldots, N\} , \tag{36}$$

of deformations of nodes, satisfying (23), (33) and (34). A deformation of the type (36) for one node is shown in Fig. 2 where $\boldsymbol{p}_\Delta = \boldsymbol{p} + 0.2\boldsymbol{n}^q$.

(3) Taking into account that the area $S(\Xi^q)$ of the domain

$$\Xi^q = e^{q1} \cup \cdots \cup e^{ql}$$

is

$$S(\Xi^q) = \frac{1}{2}(\|\boldsymbol{b}^1\| + \cdots + \|\boldsymbol{b}^l\|)$$

where $\boldsymbol{b}^1, \ldots, \boldsymbol{b}^l$ satisfy (26)–(28), the set of the displacements $\Delta\boldsymbol{p}^i, i = 1, \ldots, N$ of nodes $\boldsymbol{p}^i, \boldsymbol{p}^i \in \bar{\Gamma}, i = 1, \ldots, N$ can be defined as dependent on the distance between the nodes

$$\{\Delta\boldsymbol{p}^i = \varepsilon_i \sqrt{S(\Xi^q)}\boldsymbol{n}^i, \quad i = 1, \ldots, N\}. \tag{37}$$

To minimize functional (12), the set $\Psi_3^\varepsilon(\bar{\Gamma})$ of possible deformations (37), satisfying (33), (34) and (23), can be used.

3.6. Approximation of the variational problem

Fix a set of possible displacements $\Psi \in \{\Psi_1, \Psi_2, \Psi_3\}$. For fixed N and ε find $\boldsymbol{p}_*^1, \boldsymbol{p}_*^2, \ldots, \boldsymbol{p}_*^N$ which define a surface, such that

$$V(\bar{\Gamma}^*(\boldsymbol{p}_*^1, \boldsymbol{p}_*^2, \ldots, \boldsymbol{p}_*^N) \| \partial\Omega_1, \ldots, \partial\Omega_m) = V_0 \quad \text{and} \quad \Delta F(\bar{\Gamma}^*(\boldsymbol{p}_*^1, \boldsymbol{p}_*^2, \ldots, \boldsymbol{p}_*^N)) \geq 0$$

for each $\bar{\Gamma}_\Delta^* \in \Psi^\varepsilon(\Gamma^*)$.

The surface $\bar{\Gamma}^* = \bar{\Gamma}^*(N, \varepsilon)$ and the set of fixed solid surfaces $\partial\Omega_i, i = 1, \ldots, m$ are (N, ε) approximation of the solution of the variation Problem $\mathcal{T}$. Accuracy of the (N, ε) solution is estimated by the distance between this solution and solutions $(N, \varepsilon/2)$, $(2N, \varepsilon)$.

3.7. Iterative algorithm

The numerical method for obtaining a solution of Problem $\mathcal{T}$ is based on an iterative approach.

(1) Fix $N = N_0$, $\varepsilon = \varepsilon_0$. Start from $\boldsymbol{p}_0^1, \boldsymbol{p}_0^2, \ldots, \boldsymbol{p}_0^N$ such that $\bar{\Gamma}^0(\boldsymbol{p}_0^1, \boldsymbol{p}_0^2, \ldots, \boldsymbol{p}_0^N)$ is a triangulation of the initial surface Γ^0 which gives volume and boundary conditions.

Step 0.
- Choose a starting surface Γ^0,
- Obtain a triangulation $\bar{\Gamma}^0(\boldsymbol{p}_0^1, \boldsymbol{p}_0^2, \ldots, \boldsymbol{p}_0^N)$.

Iteratively generate a sequence $\{\boldsymbol{p}_k^1, \boldsymbol{p}_k^2, \ldots, \boldsymbol{p}_k^N\}$, such that

$$\Delta F^k = F(\bar{\Gamma}^k(\boldsymbol{p}_k^1, \boldsymbol{p}_k^2, \ldots, \boldsymbol{p}_k^N)) - F(\bar{\Gamma}^{k-1}(\boldsymbol{p}_{k-1}^1, \boldsymbol{p}_{k-1}^2, \ldots, \boldsymbol{p}_{k-1}^N)) < 0; \quad k = 1, 2, \ldots$$

(2) *Step* $k, k > 0$. Let $\bar{\Gamma}^{k-1}$ be obtained in the current $k-1$-iteration.

(2.1) Choose

$$\bar{\Gamma}_\Delta^{k-1}(\boldsymbol{p}_{k-1,\Delta}^1, \boldsymbol{p}_{k-1,\Delta}^2, \ldots, \boldsymbol{p}_{k-1,\Delta}^N) \in \Psi^\varepsilon(\bar{\Gamma}^{k-1}).$$

(2.2) Calculate

$$\Delta F = F(\bar{\Gamma}_\Delta^{k-1}) - F(\bar{\Gamma}^{k-1}).$$

If $\Delta F < 0$
then $\boldsymbol{p}_{k-1,\Delta}^1, \boldsymbol{p}_{k-1,\Delta}^2, \ldots, \boldsymbol{p}_{k-1,\Delta}^N$ are obtained in the current k-iteration.
Else
if we have compared $\bar{\Gamma}^{k-1}$ to all $\bar{\Gamma}_\Delta^{k-1} \in \Psi^\varepsilon(\bar{\Gamma}^{k-1})$ (mind that the set $\Psi \in \{\Psi_1, \Psi_2, \Psi_3\}$ is finite)
then $\bar{\Gamma}^{k-1} = \bar{\Gamma}^{k-1}(\boldsymbol{p}_{k-1}^1, \boldsymbol{p}_{k-1}^2, \ldots, \boldsymbol{p}_{k-1}^N) = \bar{\Gamma}^*(N, \varepsilon)$ is the (N, ε) solution of the Problem $\mathcal{T}$. Go to (3).

Else choose other $\bar{\Gamma}_{\Delta}^{k-1}(p_{k-1,\Delta}^{1}, p_{k-1,\Delta}^{2}, \ldots, p_{k-1,\Delta}^{N}) \in \Psi^{\varepsilon}(\bar{\Gamma}^{k-1})$ and go to (2.2).

(3) If $N = N_0$ and $\varepsilon = \varepsilon_0$,
then change parameter $\varepsilon = \varepsilon/2$ and go to (2.1) using a new value of ε,
else compare this solution to the recently obtained solution with different N and (or) ε.
Compare once more these solutions and:
- change N and (or) ε. Go to (2).
- or close the proses.

REMARK 2. The realization of the iterative procedure with $\Psi = \Psi_1$ may be considered as a relaxation method. Realization with $\Psi = \Psi_2$ and $\Psi = \Psi_3$ may be considered as a gradient method.

For the results, reported below, we have used $\Psi = \Psi_3$ in which instead of set (33) is used the set

$$\{(0, \ldots, \varepsilon_i = \pm\varepsilon, 0, \ldots, \varepsilon_j \neq 0, 0, 0), \quad 1 \leq i, j \leq N, i \neq j\} .$$

We begin the iterative process for $\varepsilon = 0.02$ and stop it for $\varepsilon = 0.00001$, keeping N and employing a remeshing procedure.

4. Test example

In this section our method is tested on the equilibrium of a sessile liquid drop on a flat horizontal plane $\partial\Omega_1$. In this configuration, according to the theorem of Wente [10], there is only one equilibrium drop, which shape is rotationally symmetric. Therefore, we may compare results of our method to the axisymmetric solutions obtained in [1–3].

Mind that for this case the Laplace equation (14), in a coordinate system (r, θ, z) and $\partial\Omega_1 = \{z = 0\}$, reduces to the ordinary differential equations (see [2])

$$\begin{aligned} \frac{d^2 r}{ds^2} &= -\frac{dz}{ds}\left(bz + C - \frac{1}{r}\frac{dz}{ds}\right) \\ \frac{d^2 z}{ds^2} &= \frac{dr}{ds}\left(bz + C - \frac{1}{r}\frac{dz}{ds}\right) \end{aligned} \tag{38}$$

for a drop profile in the (r, z) plane. Here, $r = r(s)$, $z = z(s)$, s is the arc length measured from the apex $(0, 0, z_{\text{apex}})$, C is a constant

$$C = k(0) - bz_{\text{apex}} ,$$

$k = k(s)$ is the drop curvature in the (r, z) plane.

The relevant boundary conditions are

$$r(0) = 0 , \qquad \frac{dr(0)}{ds} = 1 , \qquad \frac{dz(0)}{ds} = 0 , \qquad z(s_{\max}) = 0 , \tag{39.1}$$

$$\frac{dz(s_{\max})/ds}{dr(s_{\max})/ds} = \sqrt{1 - \chi_1^2}/\chi_1 \tag{39.2}$$

Here, Eq. (15.2) is reduced to (39.2). We then have that $\cos\varphi$ of the contact angle φ between the equilibrium free drop surface and the solid boundary is

$$\cos\varphi = -\chi_1 .$$

The drop profiles, numerically solving (38) and (39) for $b = 1$, $\chi_1 = 0$, $k(0) = 0.5$ and 1, by using a fourth-order Runge–Kutta method as in [2], are shown in Figs. 3(c) and 4(c). The contact angle φ in this examples is $\pi/2$. We have that the volume V, the height $z(0)$ and the radii $r(s_{\max})$ of the base of the drop are

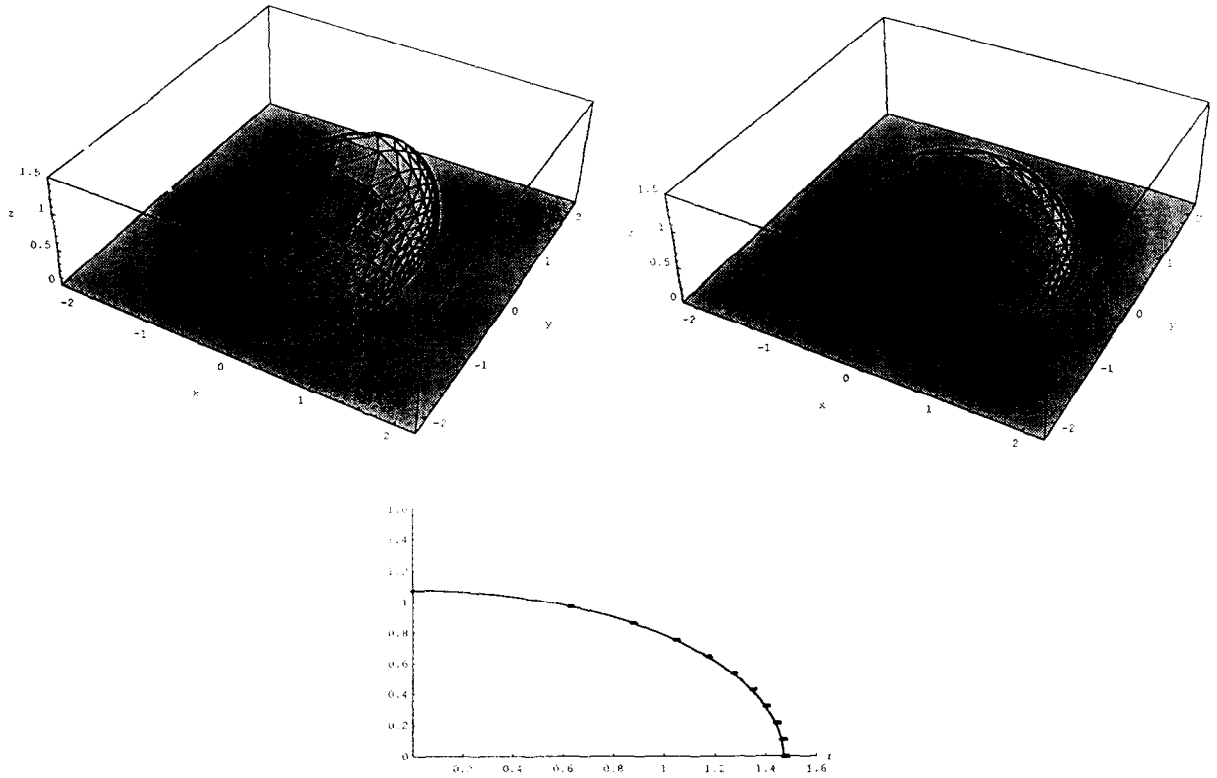

Fig. 3. Drop on a horizontal plane for $b = 1, \chi_1 = 0, V = 4.84$. (a) The triangulations of the starting surface; (b) ending drop's shape for $\varepsilon = 0.00001$; (c) with solid line—drop's profile in $(r - z)$ plane of axisymmetrical drop's shape. With points are drawing (r, z) coordinates of nodes of ending form of the drop, where axis z is drawn through the apex of the ending surface.

$$V = 4.84\,, \qquad z(0) = 1.077\,, \qquad r(s_{\max}) = 1.468 \tag{40}$$

for a drop with $k(0) = 0.5$ shown in Fig. 3(c) and

$$V = 1.25\,, \qquad z(0) = 0.767\,, \qquad r(s_{\max}) = 0.885 \tag{41}$$

for a drop with $k(0) = 1$, shown in Fig. 4(c).

Compare these drop profiles with results of the above iterative method. To illustrate the convergence and accuracy of the results of this method, let us start our iterative method by using non-symmetric surfaces Γ^0 given by the equation

$$\Gamma^0 = \left\{ x, y, z \,\middle\|\, \frac{x^2}{A} + \frac{y^2}{B} + \frac{z^2}{C} = 1\,, \quad z \geqslant 0 \right\}$$

where

$$A = \frac{r(s_{\max})}{1.3}\,, \qquad B = 1.3\,\frac{3V}{2\pi r(s_{\max})}\,, \quad C = z(0)\,,$$

$z(0)$ and $r(s_{\max})$ satisfy (40) or (41). Γ^0 is a part of a spheroid.

The triangulations $\bar{\Gamma}^0$ of the surface Γ^0 for $V_0 = 4.84$; $(V_0 = V(k(0) = 0.5))$ and $V_0 = 1.25$; $(V_0 = V(k(0) = 1))$ are shown in Figs. 3(a) and 4(a). Here

$$N = 331\,, \qquad N1 = 271\,, \qquad l = 6 \quad \text{for } q = 1, \ldots, N1\,.$$

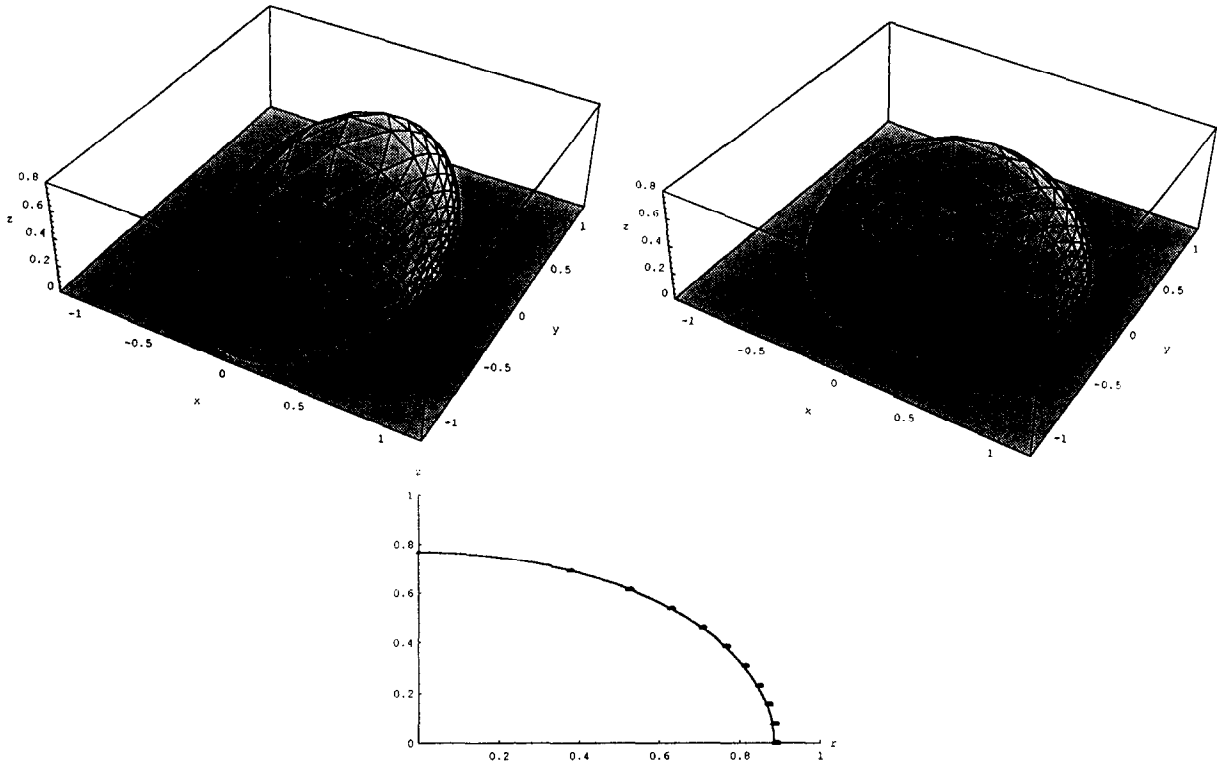

Fig. 4. Drop on a horizontal plane for $b = 1, \chi_1 = 0, V = 1.25$. (a) The triangulations of the starting surface; (b) ending drop's shape for $\varepsilon = 0.00001$; (c) with solid line—drop's profile in $(r - z)$ plane of axisymmetrical drop's shape. With points are drawing (r, z) coordinates of nodes of ending form of the drop, where axis z is drawn through the apex of the ending surface.

Numerical process starts for $\varepsilon = 0.01$. The final drop shapes are shown in Figs. 3(b) and 4(b) for $\varepsilon = 0.00001$.

In Figs. 3(c) and 4(c) with points are denoted (r, z) coordinates of $\boldsymbol{p}_*^1, \boldsymbol{p}_*^2, \ldots, \boldsymbol{p}_*^{331}$ in a cylindrical coordinate system (r, θ, z), where the axis z is drawn through the apex of the surface $\bar{\Gamma}^*(\boldsymbol{p}_*^1, \boldsymbol{p}_*^2, \ldots, \boldsymbol{p}_*^N)$. The distance between the points and the solid line in Figs. 3(c) and 4(c) shows the deviation of the surface $\bar{\Gamma}^*(\boldsymbol{p}_*^1, \boldsymbol{p}_*^2, \ldots, \boldsymbol{p}_*^N)$ from an axisymmetrical form. This illustrates the convergence and accuracy of the presented method.

5. Application of the method to a sessile-pendant drop

Consider now a liquid drop on an inclined plane $\partial\Omega_1$, hanging from a square $\partial\Omega_2$ parallel to the plane $\partial\Omega_1$. Denote by A a side of the square, by h the distance between the plane and the square, by α an angle of inclination of plane $\partial\Omega_1$. Consider the case in which virtual displacements satisfy conditions (7.1)

$$\delta \boldsymbol{r}_1 \perp \boldsymbol{n}_1 \quad \text{for } \boldsymbol{r}_1 \in \partial\Omega_1 , \tag{43}$$

and

$$\delta \boldsymbol{r}_2 = 0 \quad \text{for } \boldsymbol{r}_2 \in \partial\Omega_2 . \tag{44}$$

Parameters of this configuration are $V_0, b, \chi_1, A, h, \alpha$, as well as the square orientation.

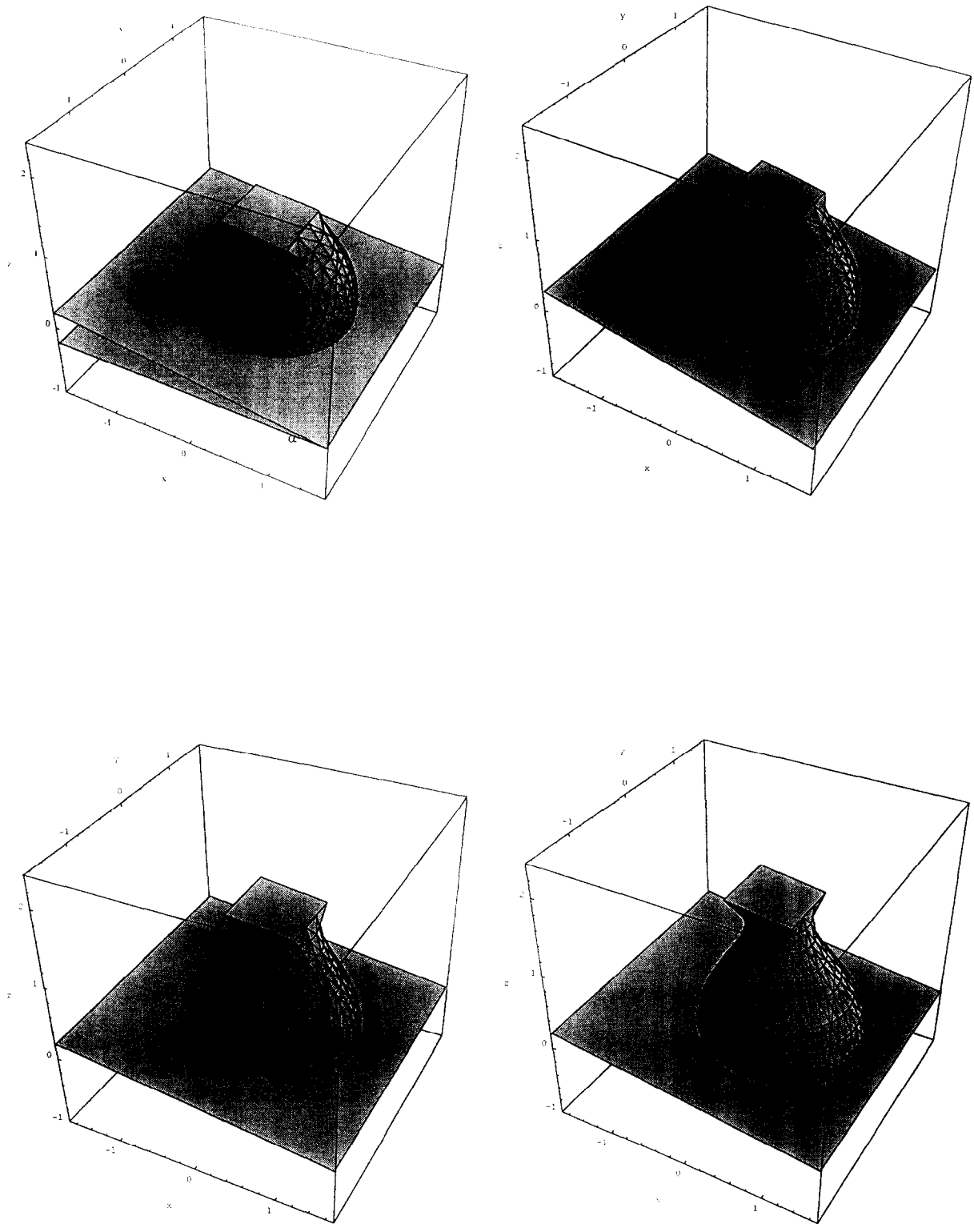

Fig. 5. Drop's shapes on inclined plane, handing from a square as function of distance h between plane and square. Square side $A = 0.93$, $V = 4.84$, $b = 1$, $\chi_1 = 0$. (a) Ending drop's shape for $h = 1.077$; (b) for $h = 1.32$; (c) for $h = 1.55$; (d) for $h = 1.69$; (e) $h = 1.71$ drop's shape at the step of the iterative process in which the drop's shape is teared.

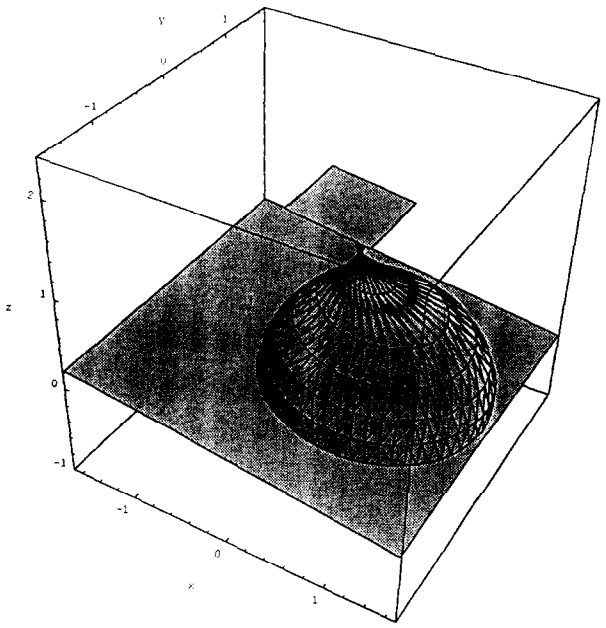

Fig. 5 (Contd.)

Fix V_0, b, A and the square orientation and obtain drop shape as a function of h, χ_1 and α. We consider the case, in which drop volume V_0 and b are identical with the volume and b of the drop of the test example with $k_1(0) = 0.5$, where $V = 4.84$, $b = 1$, two sides of the square are parallel to the line L_{hor}, $L_{\text{hor}} = \partial\Omega_1 \cap \Gamma_{\text{hor}}$, and Γ_{hor} is a horizontal plane $-\Gamma_{\text{hor}} = \{z = 0\}$, $A = 0.93$.

Start the iterative method by using a truncated pyramid Γ^0, because in the set of truncated pyramids it is easy to obtain an initial surface which gives volume and boundary conditions. Use triangulations with

$$N = 331\,, \qquad N1 = 253\,, \qquad N2 = 295\,, \qquad l = 6 \quad \text{for } q = 1, \ldots, N_1\,.$$

Firstly, fix $\chi_1 = 0$ and $\alpha = \pi/24$. The final drop shapes ($\varepsilon = 0.00001$) as a function of the distance h for $h = 1.077, 1.32, 1.55$ and 1.69 are shown in Fig. 5(a)–(d). Distance h in Fig. 5(a) is equal to the height of the sessile drop on the horizontal plane. Numerical experience shows that for each h can exist only one equilibrium drop shape. There is a critical value h^* of the distance h so that for larger values equilibrium shapes do not exist. For our case $h^* \approx 1.7$. In Fig. 5(e) is shown one of the drop shapes for $h = 1.71$, at a step of the iterative process in which the drop shape is teared. For this value of h, for an arbitrary initial shape, the iterative method is not convergent. This shows that using the iterative numerical method we can obtain critical parameters of the studied equilibrium system.

Fix now $\chi_1 = 0$ and $h = 1.32$. The final drop shapes ($\varepsilon = 0.00001$) as a function of the angle of inclination α of a plane for $\alpha = \pi/24, \pi/12$ and $\pi/8$ are shown in Fig. 5(b) and Fig. 6(a) and (b). The critical angle of inclination α^* for this case is $\alpha^* \approx \pi/7.6$. The iterative process for the angles of the inclination, larger than the critical angle α^*, is similar to the process, shown in Fig. 5(e).

REMARK 3. This case describes a mechanical system – a water drop on an iron interface in an air medium, the drop hanging from a square with a square side 2.7 mm.

Fix now $h = 1.32$ and $\alpha = \pi/24$. The final drop's shapes ($\varepsilon = 0.00001$) as a function of the contact angle φ between the equilibrium free drop surface and the inclined plane ($\cos\varphi = \chi_1$), for $\varphi = \pi/3$: ($\chi_1 = -0.5$), $\pi/2$: ($\chi_1 = 0$) and $2\pi/3$: ($\chi_1 = 0.5$), are shown in Fig. 7(a), Fig. 5(b) and Fig. 7(b).

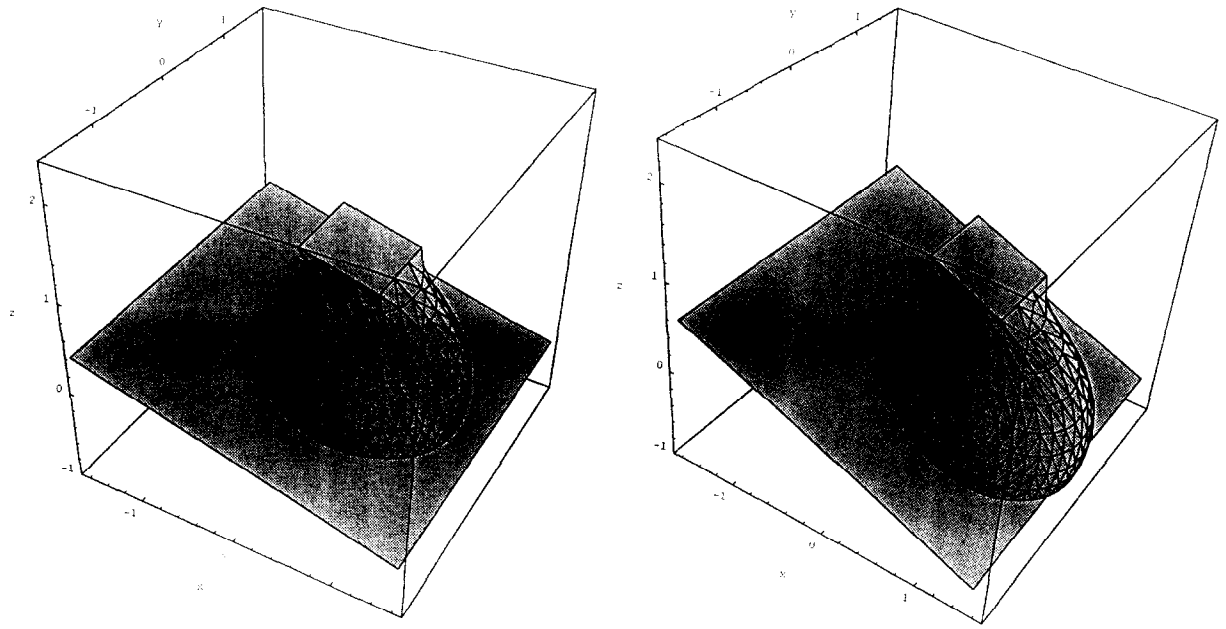

Fig. 6. The ending drop's shapes as function of angle α of inclination of plane, $\chi_1 = 0$. (a) For $\alpha = \pi/12$; (b) for $\alpha = \pi/8$.

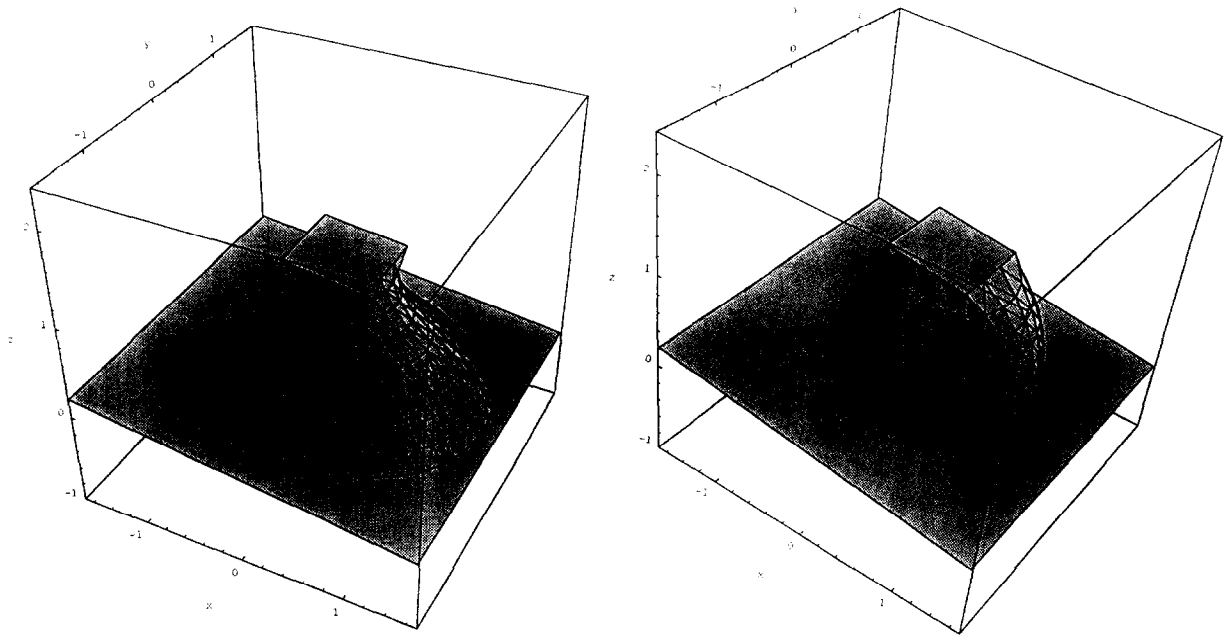

Fig. 7. The ending drop's shapes as function of contact angle φ between equilibrium free drop surface and inclined plane, $h = 1.32$, $\alpha = \pi/24$. (a) For $\varphi = \pi/3$; (b) for $\varphi = 2\pi/3$.

6. Concluding remarks

A new variation approach to Plato's problem is described in the present work. The peculiarity of this approach is that virtual displacements in physical 3-D space are directly simulated. The method gives a possibility to approximate not the entire drop volume, as in the classical FEM case. There we approximate at each step only the volume of the 'boundary region'. The scheme of the realization of the method is a new one. The technique of this method may be considered as a hybrid boundary-finite

element method. The consideration of a test example and an application of the method to solve 'sessile-pendant' drops shows that the presented iterative method is effective to obtain the equilibrium shapes of liquid drops, including non-axisymmetrical shapes. Moreover, the method gives good results for different boundary conditions. And it is applicable to mechanical systems, whose energy consists of volume and surface terms.

References

[1] J.F. Padday, The profiles of axially symmetric menisci, Phil. Trans. R. Soc. Lond. A 269 (1971) 265–293.
[2] S. Hartland and R.W. Hartley, Axisymmetric Fluid Interfaces (Elsevier, Amsterdam, 1976).
[3] B.G. O'Brien, On the shape of small sessile and pendant drops by singular perturbation techniques, J. Fluid Mech. 233 (1991) 519–537.
[4] P.J. Shopov and I.Bl. Bazhlekov, Numerical method for viscous hydrodynamic problems with dynamic contact lines, Comput. Methods Appl. Mech. Engrg. 91 (1991) 1157–1172.
[5] B. Dusan V. and R.T.-P. Chow, On the ability of drops or bubbles to stick to non-horizontal surfaces of solids, J. Fluid Mech. 137 (1983) 1–29.
[6] R.A. Broun, F.M. Orr, Jr and L.E. Scriven, Static drops on an inclined plane: Analysis by the finite element method, J. Colloid Interface Sci. 73 (1980) 76–87.
[7] S.D. Iliev, On a modification of a local variations method, Vestnik Mosk. Univ., ser. Num. Math. and Cybernetics 4 (1991) 54–60.
[8] R. Finn, Equilibrium Capillary Surfaces (Springer, Berlin, 1986).
[9] L.D. Landay and E.M. Lifshitz, Fluid Mechanics (Pergamon, Oxford, 1987).
[10] H.C. Wente, The symmetry of sessile and pendant drops, Pacific J. Math. 88 (1980) 387–397.